

Spectral, optical, and thermal studies of pure and Zn(II)-doped L-histidine hydrochloride monohydrate (LHHC) crystals

C. Alosious Gonsago · Helen Merina Albert ·
R. Umamaheswari · A. Joseph Arul Pragasam

Received: 18 July 2011 / Accepted: 3 August 2011 / Published online: 17 August 2011
© Akadémiai Kiadó, Budapest, Hungary 2011

Abstract The influence of doping the transition metal Zn(II) on the growth, spectral, optical, and thermal properties of L-histidine hydrochloride monohydrate (LHHC) crystals grown by slow solvent evaporation method has been investigated. Structural characterizations of the grown crystals were carried out by single crystal X-ray diffraction analysis and it shows slight structural changes as a result of doping. The FT-IR spectral study reveals the presence of various functional groups and confirms the slight distortion of the structure of the crystals due to doping. The energy dispersive X-ray analysis reveals the incorporation of Zn(II) in the crystalline matrix of LHHC crystal. The UV–Vis spectral study was carried out to analyze the optical transmittance of the grown crystals and found that the transmittance is very high in the visible and UV regions for both pure and doped crystals. The second harmonic generation (SHG) for the grown crystals was confirmed by Nd:YAG laser. The scanning electron microscopy reveals the presence of defect centers and crystal voids. The thermal stability and purity of the grown crystals were analyzed by thermogravimetry, differential thermal analysis, and differential scanning calorimetry techniques.

Keywords XRD · UV · FT-IR · Energy dispersive X-ray analysis (EDAX) · TG · DTA · DSC

Introduction

In recent years, nonlinear optical (NLO) materials have attracted considerable attention than other materials due to their applications in laser technology, optical communications, optical switching, data storage, optical mixing, and electro-optic applications [1–4]. In pure organic crystals, molecules are often coupled by rather weak van der Waals forces or hydrogen bonding which results in poor mechanical and thermal stability. To overcome these problems, semi-organic hybrid compounds are explored for nonlinear applications. Complexes of amino acids with inorganic salts have been of immense interest as they share the properties of both organic and inorganic materials such as high laser damage threshold, optical transparency, and high efficiency [5–7]. In semi-organic materials, the organic molecule is stoichiometrically bound to a suitable inorganic or metal ion, thereby improving the hardness and thermal stability of the specimen. It is interesting to note that all amino acids except glycine have chiral symmetry and crystallize in the non-centrosymmetric space group [8]. Moreover, the amino acids are dipolar in nature and the molecules possess an electron donor group and an electron acceptor group. This leads to large second order optical nonlinearity arising out of intramolecular charge transfer between the two groups opposite in nature. Due to this dipolar nature, amino acids have been considered potential candidates for NLO applications [9–11].

The basic amino acid L-histidine has been widely studied with the discovery of promising nonlinear optical NLO material L-histidine tetrafluoroborate [12]. Recently,

C. Alosious Gonsago
Department of Physics, A. J. College of Engineering, Chennai
603 103, India

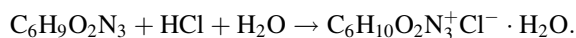
H. M. Albert · R. Umamaheswari ·
A. Joseph Arul Pragasam (✉)
Department of Physics, Sathyabama University,
Chennai 600 119, India
e-mail: drjosephsu@gmail.com

several new salts of L-histidine have been reported with excellent NLO properties [13–15]. L-Histidine hydrochloride monohydrate (LHHC) is one such semi-organic material suitable for NLO applications [16]. The Zn-doped III–V semiconductor layers have been proposed in the recent years as efficient materials suitable for opto-electronic devices [17]. Spectral, optical, thermal, and microscopic analyses are useful methods for materials characterization. Hence, many authors have used these techniques for various materials characterization [18–22]. In order to extend the works made on LHHC crystal and to ascertain the effect of doping on its properties, this study has been under taken. In this study, we have used Zn(II), a transition metal for doping the LHHC crystal. The crystal growth, X-ray diffraction (XRD), energy dispersive X-ray analysis (EDAX), FT-IR, UV–Visible absorption, second harmonic generation (SHG), scanning electron microscopy (SEM), and TG–DTA–DSC analyses of pure and Zn(II)-doped LHHC crystals are systematically studied.

Experimental

Crystal growth

Analar reagent (AR) grade of L-histidine and hydrochloric acid were used for the growth of single crystals. The LHHC crystal was grown by dissolving equimolar ratio of L-histidine and hydrochloric acid in doubled distilled water. The reaction that takes place in this process is as follows:



The prepared solution was constantly stirred for about 6 h using magnetic stirrer to obtain homogeneous mixture over the entire volume. By heating the mixture to dryness below an optimum temperature of 55 °C in a temperature controllable water bath, colorless tiny crystalline samples were obtained and were used for the growth of LHHC single crystal. To ensure high purity, the material was purified by successive crystallization. The synthesized compound was thoroughly dissolved in double distilled water to form saturated solution. Then, the solution was filtered twice to remove the suspended impurities using micro-Whatman filter paper and kept in a borosil beaker covered with porous paper to facilitate the evaporation of the solvent. To maintain constant growth rate, it was placed in a constant temperature water bath at 32 °C. To get Zn(II)-doped LHHC, 2 wt% of Zn(II) in the form of ZnSO_4 was added to the saturated solution of L-histidine hydrochloric acid and the same method was followed as that of pure LHHC. The crystals of optimum size were obtained after a period of 25 days. The photographs of as-grown crystals of pure and Zn(II)-doped LHHC are shown in Fig. 1.

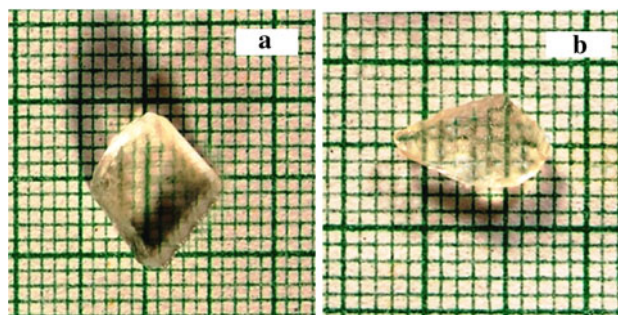


Fig. 1 Photographs of **a** pure and **b** Zn(II)-doped LHHC crystals

Results and discussion

Single crystal XRD study

In order to identify the lattice parameters of the grown crystals, single crystal XRD study was performed using ENRAF-NONIUS CAD4 diffractometer with Mo- $K\alpha$ radiation source of wavelength 0.717 Å. The single XRD data shows that both pure and Zn(II)-doped LHHC crystals are orthorhombic in structure with the space group $P2_12_12_1$. It is well known that $P2_12_12_1$ is a non-centrosymmetric space group hence satisfying the basic and essential material requirement for the second order NLO activity of the compound. The lattice parameters of pure LHHC are $a = 15.285$ Å, $b = 8.884$ Å, $c = 6.876$ Å, and $V = 933.71$ Å³. The observed lattice parameters are in good agreement with reported values [23]. The molecular structure of LHHC crystal is provided in Fig. 2. The XRD data of the pure LHHC is compared with the observed lattice parameters of Zn(II)-doped LHHC crystal and is presented in Table 1. A marginal increase in the lattice parameters and volume has been observed for the Zn(II)-doped LHHC crystal in comparison with the pure LHHC crystal. This may be due to the inclusion of Z(II) in the lattice of pure LHHC crystal.

FT-IR spectral analysis

In order to identify the presence of various functional groups in the grown crystal, FT-IR spectral analysis was performed in the frequency region 450–4000 cm^{-1} using Perkin-Elmer spectrometer by KBr pellet technique. The

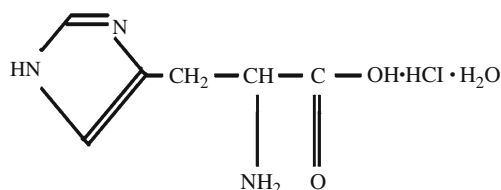
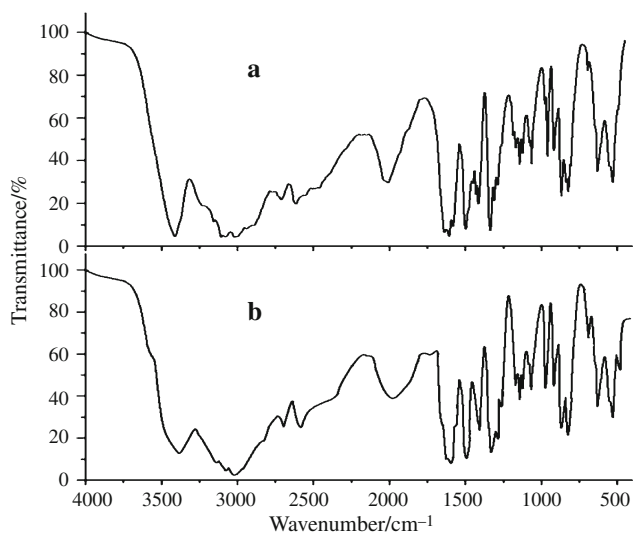


Fig. 2 Molecular structure of LHHC crystal

Table 1 Single crystal XRD data of pure and Zn(II)-doped LHHHC crystals

Sample	Cell parameters/Å	Volume/Å ³	Space group
Pure LHHHC	$a = 15.285$	933.71	$P2_12_12_1$
	$b = 8.884$		
	$c = 6.876$		
Zn(II)-doped LHHHC	$a = 15.354$	936.59	$P2_12_12_1$
	$b = 8.896$		
	$c = 6.857$		

**Fig. 3** FT-IR spectra of **a** pure and **b** Zn(II)-doped LHHHC crystals

recorded spectra of both the crystals are shown in Fig. 3. The assignments of various functional groups are listed in Table 2.

The spectral bands are interpreted and compared with the known spectra of the functional groups [24–26]. The FT-IR spectra of pure LHHHC shows a strong and intense peak at 3411 cm^{-1} , which is ascribed to O–H stretching of carboxylic acid and the presence of water molecule in the crystal. The peak at 3157 cm^{-1} is attributed to the existence of NH group in amine functionality. The aromatic and aliphatic C–H stretching vibrations are resolved at 3019 and 2712 cm^{-1} . The strong and broad peak at 1637 cm^{-1} is due to the presence of unprotected C=O group. The peaks at 1580 and 1414 cm^{-1} are assigned to asymmetric and symmetric stretching vibration of COO^- . The strong peak at 1143 cm^{-1} is attributed to aromatic C–N stretching vibration. The broad band from 3200 to 2100 cm^{-1} is assigned to asymmetric and symmetric stretching vibrations of the O–H, N–H, and C–H bands. The torsional N–H oscillations of NH_3^+ are observed at 530 cm^{-1} . A very slight shift in some of the characteristic

vibrational frequencies is observed in the FT-IR spectra of doped crystal, due to the doping with Zn(II). The important bands that support our interpretations are listed in Table 2.

EDAX analysis

EDAX is a microanalytical technique, used to get the information regarding the elemental composition of the grown crystals. In this study, the grown crystals were analyzed by FEI QUANTA 200F energy dispersive X-ray microanalyzer. The spectra obtained by EDAX analysis for the pure and Zn(II)-doped LHHHC crystals are shown in Fig. 4. The weight percentage (wt%) of C, N, O, Cl, and Zn(II) as obtained from EDAX analysis for both the crystals are compared and presented in Table 3. From the experimental data, the presence of Zn(II) in the doped crystal can be easily identified.

UV–Vis spectral analysis

The UV–Vis spectral study was performed for the grown crystals to know the transmittance range and also to identify the suitability of the crystals for optical applications. The transmittance spectra were recorded with a Varian Carry-5E UV–Vis spectrophotometer in the wavelength range 200 – 1000 nm for both the pure and doped crystals. The recorded transmittance spectra for both the crystals are shown in Fig. 5. From the transmittance spectra, it is observed that the grown crystals are found to be transparent in the entire UV and visible regions, which will enable the crystals to be excellent materials for SHGs and optoelectronic applications. The optical transmission is not altered much due to the doping. A sharp fall in transmittance is observed in the spectra of the pure LHHHC at 231 nm and this corresponds to the lower cut-off wavelength or fundamental absorption of the crystal. Also, it is observed that the lower cut-off wavelength is not altered in the case of Zn(II) doping.

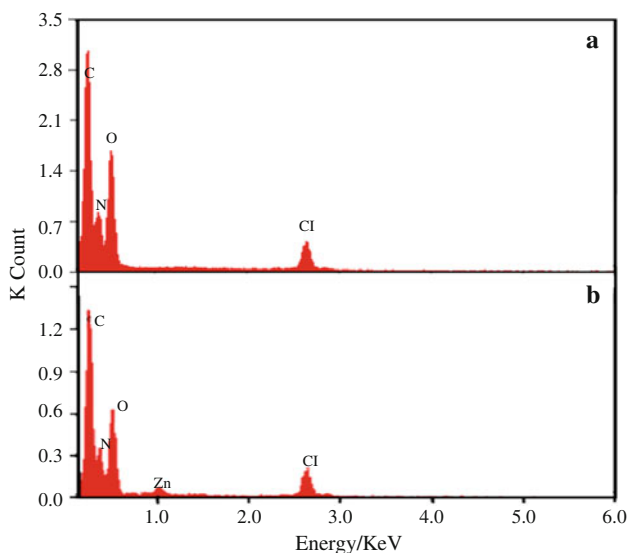
The optical transmittance spectral study is also useful in understanding the electronic structure of the band gap of the grown crystals. The study of absorption edge is crucial in association with the theory of electronic structure, as it leads to the prediction of whether the band structure is affected in the vicinity of the band extreme. Hence, it is essential to calculate the magnitude and the nature of optical energy band gap of both the pure and doped LHHHC crystals. The optical energy gaps of the grown crystals are determined from the transmittance spectra using Tauc relation [27, 28]. According to Tauc relation, the absorption coefficient α for a material is given by,

$$\alpha h\nu = A(h\nu - E_g)^n$$

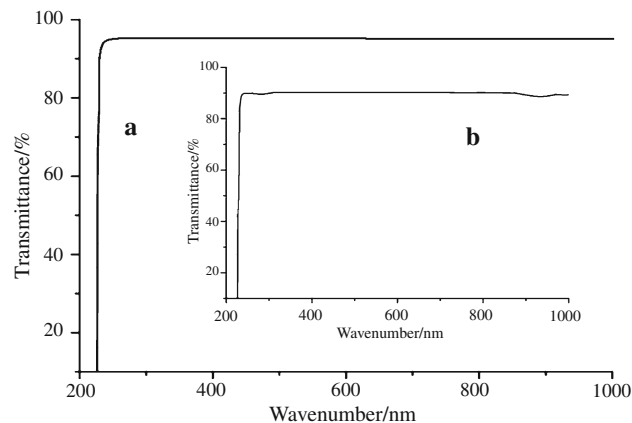
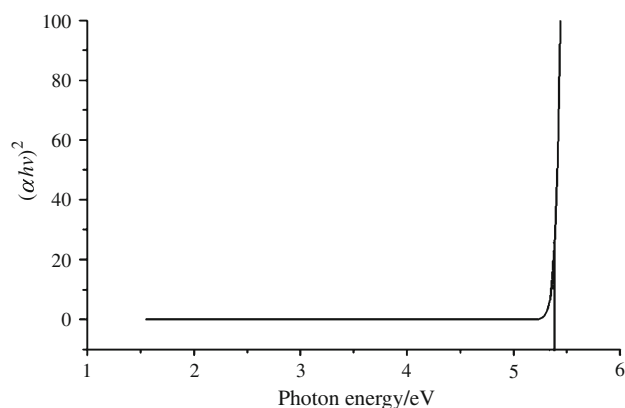
where A is a constant which varies with transitions, E_g is the band gap of the material, and n is an index which can

Table 2 FT-IR frequency assignments for pure and Zn-doped LHHC crystals

Pure/cm ⁻¹	Zn-doped/cm ⁻¹	Assignments
3411	3409	O–H stretch of water
3157	3148	NH stretching
3106	3088	NH ₃ ⁺ stretching
3019	3011	Aromatic C–H stretching
2712	2705	Aliphatic C–H stretching
2009	2003	Overtone and combination modes
1637	1631	C=O stretching
1606	1603	Asymmetric bending of NH ₃ ⁺
1580	1566	Asymmetric stretching of COO ⁻
1497	1499	Symmetric bending of NH ₃ ⁺
1414	1416	Symmetric stretching of COO ⁻
1143	1141	C–N stretching
1064	1086	C–O Stretching of carbonyl group
959	961	Ring asymmetric stretching
867	870	Ring symmetric stretching
834	839	C–C–O stretching
630	631	Ring deformation
530	536	Torsional oscillation of NH ₃ ⁺

**Fig. 4** EDAX spectra of **a** pure and **b** Zn(II)-doped LHHC crystals**Table 3** EDAX quantification data for the grown crystals

Element	Pure LHHC/wt%	Zn(II)-doped LHHC/wt%
C	49.78	48.99
N	23.49	23.03
O	19.98	19.70
Cl	06.75	06.56
Zn(II)	–	01.72

**Fig. 5** UV–Vis optical spectra of **a** pure and **b** Zn(II)-doped LHHC crystals**Fig. 6** Plot of $(\alpha hv)^2$ versus photon energy hv

have the values 1/2, 3/2, 2, or 3 depending on the nature of the electronic transitions. Here, the value of n is assigned as 1/2 for an allowed direct transition. From the transmittance spectra, a graph is drawn between hv and $(\alpha hv)^2$ and is displayed in Fig. 6. The band gap energy of both the crystals is evaluated by exploring a straight line in the linear region of the graph at $(\alpha hv)^2 = 0$ [29, 30]. The band gap energies for the pure and Zn(II)-doped LHHC crystals are almost same and the calculated value is 5.37 eV.

Kurtz and Perry SHG test

The SHG efficiencies of pure and Zn(II)-doped LHHC crystals were measured by the Kurtz and Perry powder technique [31]. In this technique, the grown crystals were grounded into fine microcrystalline powder and densely packed between two transparent glass slides. An Nd:YAG laser operating at a fundamental wavelength 1064 nm with 8 ns pulse width and 10 Hz pulse rate was used as an optical source. The laser beam was made to fall normally on the powdered samples through a filter. The emission of

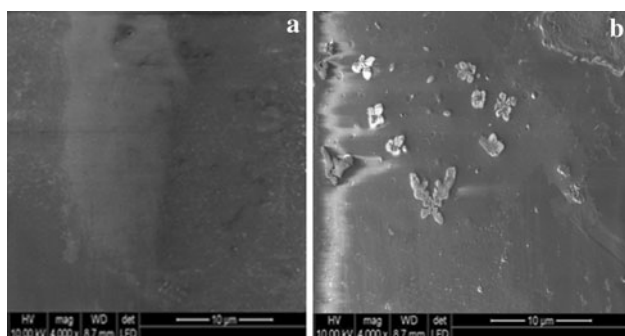


Fig. 7 SEM images of **a** pure and **b** Zn(II)-doped LHC crystals

second harmonic signal was confirmed by the emission of green radiation from both the samples.

SEM analysis

SEM provides useful information regarding the surface morphology, chemical composition, and crystalline structure of a sample. This study is also useful in finding the presence of any imperfections in the grown crystals. The SEM images of pure and Zn(II)-doped LHC are shown in Fig. 7. The image of pure crystal shows that the surface is smooth and free from any inclusions and scatter centers. But, the image of doped LHC crystal shows the presence of some visible inclusions on its surface. These visible inclusions are due to the presence of dopant in the crystal. Hence, the surface morphology of the pure LHC crystal is affected by the presence of dopant.

Thermal analyses

The thermogravimetry (TG), differential thermal analysis (DTA), and differential scanning calorimetry (DSC) techniques were employed to identify the phase transition, different stages of decomposition, and melting point of the grown crystals [32]. The TG and DTA analyses for the grown crystals were carried out using the instrument NETZSCH STA 409 C/CD. An alumina (Al_2O_3) crucible was used for heating the samples in nitrogen atmosphere at the heating rate of $10\text{ }^\circ\text{C}/\text{min}$ in the temperature range $20\text{--}1200\text{ }^\circ\text{C}$. The simultaneously recorded TG and DTA curves of both the pure and Zn(II)-doped LHC crystals are displayed in Fig. 8. The TG curve of pure LHC shows a sharp weight loss of about 11% in the temperature range $150\text{--}165\text{ }^\circ\text{C}$. This is due to the loss of water of crystallization in the compound. This is followed by a major weight loss of about 72% occurring in two stages between 210 and $1200\text{ }^\circ\text{C}$. The weight loss in these stages may be due to the decomposition and volatilization of the material. The initial mass of the compound subjected to the analysis was

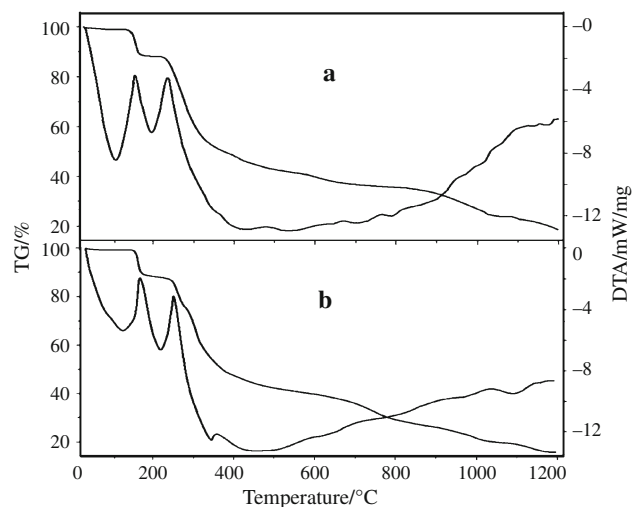


Fig. 8 TG–DTA curves of **a** pure and **b** Zn(II)-doped LHC crystals

10.25 mg and the final mass left out after the analysis was only 9.75% of the initial mass which indicates bulk decomposition of the compound. But, in the case of Zn(II)-doped crystal, the first stage of weight loss occurs in the temperature range $160\text{--}170\text{ }^\circ\text{C}$ and the next stage of weight loss occurs at around $230\text{ }^\circ\text{C}$.

The DTA curve of pure LHC shows an endothermic peak at about $155\text{ }^\circ\text{C}$ which is due to the loss of lattice water. It is followed by another peak at $245\text{ }^\circ\text{C}$ which indicates the major decomposition of the material and this corresponds to the melting point of the pure LHC. Meanwhile, the DTA curve of doped crystal shows peaks at about 168 and $255\text{ }^\circ\text{C}$ and this may be attributed to the removal of lattice water and decomposition of the doped crystal. Hence, the TG and DTA studies clearly indicate that the melting point of the pure LHC is significantly increased from 245 to $255\text{ }^\circ\text{C}$ with the inclusion of Zn(II) in the LHC crystal.

The DSC analysis was also performed for both the crystals in the temperature range $40\text{--}250\text{ }^\circ\text{C}$ at a heating rate of $10\text{ }^\circ\text{C}/\text{min}$ in the nitrogen atmosphere using the instrument NETZSCH DSC 204. The typical DSC curves of both the crystals are shown in Fig. 9. The DSC curves display the same changes shown by TG and DTA curves. The DSC curve of pure LHC is smooth up to $130\text{ }^\circ\text{C}$ and then shows two sharp endothermic peaks at 160 and $252\text{ }^\circ\text{C}$. The first peak is due to the removal of weakly entrapped lattice water and the second peak is due to the decomposition of the compound. The DSC curve of the doped crystal also shows two endothermic peaks which are slightly shifted and appear at 171 and $260\text{ }^\circ\text{C}$. Hence, it is interesting to observe that the melting point of the pure LHC crystal has significantly increased with the inclusion of Zn(II) dopant in the crystalline matrix of the LHC crystal.

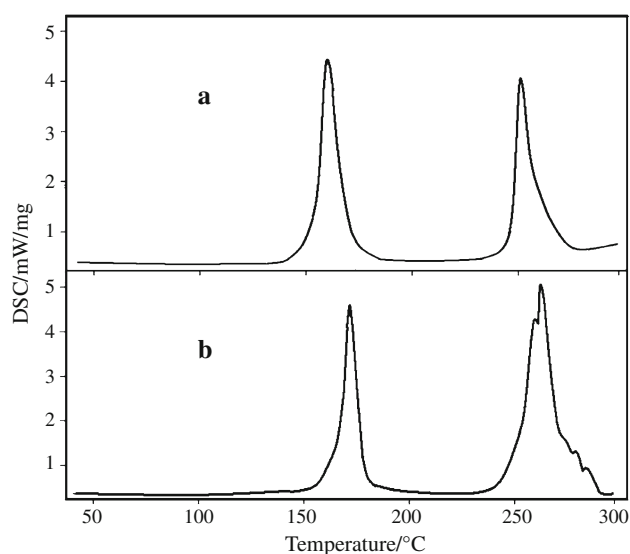


Fig. 9 DSC curves of **a** pure and **b** Zn(II)-doped LHHC crystals

Conclusions

In this study, pure and transition metal Zn(II)-doped LHHC crystals were grown by slow solvent evaporation method at room temperature in a period of 25 days. The single crystal XRD study confirms that the grown crystals belong to orthorhombic system with the space group $P2_12_12_1$. A close observation of the crystallographic data shows a marginal increase in the lattice parameters and volume for the doped crystal. The presence of various functional groups and the modes of vibrations were identified by FT-IR spectroscopy. The incorporation of Zn(II) in the doped crystal is confirmed by EDAX analysis. The UV-Vis spectral study shows that the optical transmittance is very high for both the crystals in the entire UV and visible regions. The transparency is not affected much by the incorporation of dopant. The optical band gap energies for both the crystals are found to be almost same and the estimated value is 5.37 eV. The SEM analysis shows the surface morphology of the grown crystals. The NLO property is confirmed by SHG test. The TG, DTA, and DSC studies reveal that the melting point of the pure LHHC is significantly increased as a result of Zn(II) doping.

References

- Madhurambal G, Mariappan M, Mojumdar SC. Thermal, UV and FTIR spectral studies of urea-thiourea zinc chloride single crystal. *J Therm Anal Calorim.* 2010;100:853–6.
- Verma S, Singh MK, Wadhavan VK, Suresh CH. Growth morphology of zinc tris(thiourea)sulphate crystals. *J Phys.* 2000;54: 879–88.
- Ravi Kumar SM, Melikechi N, Selvakumar S, Sagayaraj P. Growth and characterization of nonlinear optical bimetallic thiocyanate complex of MCCTC crystal. *J Cryst Growth.* 2009;311:2454–8.
- Ramajothi J, Danuskodi S. Crystal growth, thermal and optical studies on a semiorganic nonlinear optical material for blue-green laser generation. *Spectrochim Acta A.* 2007;68:1213–9.
- Kandasamy A, Siddeswaran R, Murugakoothan P, Suresh Kumar P, Mohan R. Synthesis, growth and characterization of L-proline cadmium chloride monohydrate (L-PCCM) crystals—a new nonlinear optical material. *Cryst Growth Des.* 2007;7:183–6.
- Sun GH, Sun XT, Sun ZH, Wang XQ, Liu XJ, Zhang GH, Xu D. Growth and characterization of a nonlinear optical crystal: L-histidine trifluoroacetate. *J Cryst Growth.* 2009;311:3904–10.
- Danuskodi S, Vasantha K, Mary PAA. Structural and thermal characterization of a semiorganic NLO material: L-alanine cadmium chloride. *Spectrochim Acta A.* 2007;66:637–42.
- Ittyachan Reena, Jesu Raja SX, Rajasekar SA, Sagayaraj P. Crystallization and characterization of L-histidinium perchlorate single crystal. *Mater Chem Phys.* 2005;90:10–5.
- Lydia Caroline M, Kandasamy A, Mohan R, Vasudevan S. Growth and characterization of dichloro bis L-proline Zn(II): a semiorganic nonlinear optical crystal. *J Cryst Growth.* 2009;311: 1161–5.
- Ramachandra Raja C, Gokila G, Antony Joseph A. Growth and spectroscopic characterization of a new organic nonlinear optical crystal: L-alaninium succinate. *Spectrochim Acta A.* 2009;72: 753–6.
- Aruna S, Bhagavannarayana G, Sagayaraj P. Investigation on the physicochemical properties of nonlinear optical single crystal: L-histidinium dinitrate. *J Cryst Growth.* 2007;304:184–90.
- Marcy HO, Rosker MJ, Warren LF, Cunningham PH, Thomas CA. L-histidine tetrafluoroborate: a solution-grown semiorganic crystal for nonlinear frequency conversion. *Opt Lett.* 1995;20(3): 252–4.
- Madhavan J, Aruna S, Praba K, Julius JP, Jinson J, Joseph P, Selvakumar S, Sagayaraj P. Growth and characterization of novel NLO crystal L-histidine hydrofluoride dihydrate (LHHF). *J Cryst Growth.* 2006;293:409–14.
- Petrosyan HA, Karapetyan HA, Petrosyan AM. L-Histidine nitrates. *J Mol Struct.* 2006;794:160–7.
- Jayaraman R, Sivasubramanian D. Optical and microhardness studies of semiorganic nonlinear optical material: L-histidine tetrafluoroborate. *Cryst Res Technol.* 2003;38:986–91.
- Madhavan J, Aruna S, Thomas PC, Vimalan M, Rajasekar SA, Sagayaraj P. Growth and characterization of L-histidine hydrochloride monohydrate single crystals. *Cryst Res Technol.* 2007;42: 59–64.
- Parthiban S, Murali S, Madhurambal G, Meenakshisundaram P, Mojumdar SC. Effect of zinc(II) doping on thermal and optical properties of potassium hydrogen phthalate (KHP) crystals. *J Therm Anal Calorim.* 2010;100:751–6.
- Madhurambal G, Ramasamy P, Anbusrinivasan P, Vasudevan G, Kavitha S, Mojumdar SC. Growth and characterization studies of 2-bromo-40-chloro-acetophenone (BCAP) crystals. *J Therm Anal Calorim.* 2008;94:59–62.
- Mojumdar SC, Madhurambal G, Saleh MT. A study on synthesis and thermal, spectral and biological properties of carboxylato-Mg(II) and carboxylato-Cu(II) complexes with bioactive ligands. *J Therm Anal Calorim.* 2005;81:205–10.
- Anbusrinivasan P, Madhurambal G, Mojumdar SC. *p-N,N*-dimethylaminobenzaldehyde (DAB) grown by solution technique using CCl₄ as growth medium. *J Therm Anal Calorim.* 2009; 96:111–5.
- Madhurambal G, Mojumdar SC, Hariharan S, Ramasamy P. TG, DTC, FT-IR and Raman spectral analysis of Zn/Mg

- ammonium sulfate mixed crystals. *J Therm Anal Calorim.* 2004;78:125–33.
22. Muthu K, Bhagavannarayana G, Chandrasekaran C, Parthiban S, Meenakshisundaram SP, Mojumdar SC. Os(VIII) doping effects on the properties and crystalline perfection of potassium hydrogen phthalate (KHP) crystals. *J Therm Anal Calorim.* 2010;100:793–9.
 23. Oda K, Koyama H. A refinement of the crystal structure of histidine hydrochloride monohydrate. *Acta Crystallogr B.* 1972;28:639–42.
 24. Bellamy LJ. *The infrared spectra of complex molecules.* 3rd ed. New York: Wiley; 1975.
 25. Herzberg G. *Infrared and Raman spectra of polyatomic molecules.* 1st ed. New York: Van Nostrand Reinhold; 1945.
 26. Rao CNR. *Chemical application of infrared spectroscopy.* 2nd ed. New York: Academic Press; 1963.
 27. Tauc J. *Amorphous and liquid semiconductors.* New York: Plenum press; 1974.
 28. Krishnakumar V, Sivakumar S, Nagalakshmi R, Bhuvanewari S, Rajaboopathi M. Effect of doping an organic molecule ligand on TGS single crystals. *Spectrochim Acta A.* 2008;71:480–5.
 29. Aneesh PM, Krishna KM, Jayaraj MK. Hydrothermal synthesis and characterization of undoped and Eu doped $ZnGa_2O_4$ nanoparticles. *J Electrochem Soc.* 2009;156:33–6.
 30. Fochs PD. The measurement of the energy gap of semiconductors from their diffuse reflection spectra. *Proc Phys Soc Lond.* 1956; B69:70–5.
 31. Kurtz SK, Perry TT. A powder technique for the evaluation of non-linear optical materials. *J Appl Phys.* 1968;39:3798–813.
 32. Joseph Prakash JT, Vijayan N, Kumararaman S. Growth and characterization studies on glycine barium dichloride single crystals for NLO applications. *Spectrochim Acta A.* 2008;71:1250–2.